Available online at www.eccomasproceedia.org
Eccomas Proceedia COMPDYN (2025) 1362-1369

ECCOMAS
Proceedia

COMPDYN 2025
10th ECCOMAS Thematic Conference on
Computational Methods in Structural Dynamics and Earthquake Engineering
M. Papadrakakis, M. Fragiadakis (eds.)
Rhodes Island, Greece, 15-18 June 2025

CIRCULARITY THROUGH REPAIR ACTIONS IN HEAVILY DAMAGED RC SUBSTANDARD COLUMNS

Özgür Yurdakul[1], Petr Vnenk[2], Ladislav Routil[1], Bohumil Culek[1], and Özgür Avşar[3]

[1]University of Pardubice
Pardubice, Czech Republic
e-mail: {ozgur.yurdakul,ladislav.routil,culek}@upce.cz

[2] Sprava Zeleznic
Prague, Czech Republic
e-mail: vnenkp@spravazeleznic.cz

[3] Eskişehir Technical University
Eskişehir, Türkiye
e-mail: ozguravsar@eskisehir.edu.tr

Abstract. *Earthquake-resilient construction principles are often compromised by the substandard configuration and detailing of RC buildings. Depending on the feasibility and technical constraints, post-earthquake urban transformation efforts frequently require the repair of damaged structural members or reconstruction. Rebuilding damaged reinforced concrete (RC) buildings, rather than extending their lifespan through structural repair, is estimated to have a significant impact on the environment, circular economy, and sustainability due to the need for demolition, debris removal, and reconstruction. Consequently, this study investigates the structural repair of pre-damaged RC columns with substandard configurations -characterized by low-strength concrete, plain round bars, and nonconforming reinforcement details- using carbon-fiber-reinforced polymers (CFRPs). Due to the difference in the lap-splice, hook detail in the longitudinal reinforcement, and axial load ratio of the RC columns, tested RC columns were exposed various types of structural damage. After the attainment of their heavy damage state, including flexural failure with significant reinforcement slip, and axial damage (such as concrete crushing, and reinforcement buckling), damaged RC columns were repaired using externally wrapped CFRP sheets. The repair process successfully restored the load-carrying capacities of the RC columns. Moreover, the axial failure mode, characterized by severe cracks and concrete crushing observed in the reference specimen, was effectively mitigated in the repaired specimens through the application of CFRP.*

Keywords: Circularity, Repair, Axial Failure, CFRP, Column

ISSN:2623-3347
Peer-review under responsibility of the organizing committee of COMPDYN 2025.
doi: 10.7712/120125.12494.24362

1 INTRODUCTION

Structural elements are expected to exhibit ductile behavior under loading. Modern design codes provide guidelines to ensure ductility in structural components. However, many reinforced concrete (RC) buildings in developing countries suffer from significant deficiencies that can lead to premature failure. These shortcomings often stem from poor material quality (e.g., low-strength concrete, plain round bars), inadequate detailing, and poorly regulated construction practices. Such deficiencies can result in brittle failure, severely compromising structural integrity, reducing energy dissipation capacity, and leading to sudden strength and stiffness degradation [1, 2, 3]. Since localized damage can escalate into global failure, evaluating substandard structural components is crucial to prevent total collapse. Field investigations and laboratory studies highlight that deficient RC columns are among the most vulnerable elements in moment-resisting frames [4, 5, 6]. Consequently, extensive experimental research has been conducted on the cyclic behavior of RC columns [7, 8, 9]. Given that premature column failure significantly affects seismic performance, fiber-reinforced polymer (FRP) strengthening techniques have gained substantial attention [10]. In cases where demolishing damaged structures is not feasible due to economic constraints, repairing RC columns offers a practical alternative to restoring building functionality.

While design codes prioritize life safety over preventing damage, significant economic losses often follow seismic events. For instance, the 2010–2011 Canterbury earthquakes in New Zealand caused insured losses of approximately NZ$30 billion, nearly 10% of GDP [11]. The 2009 L'Aquila earthquake in Italy resulted in 309 fatalities and an estimated loss of $566 million [12]. The 2011 Van, Turkey earthquake caused economic losses around $2.9 billion [13], while the 2023 Maraş-Türkiye earthquake had an estimated cost exceeding $103 billion [14]. Given the high reconstruction cost, repairing heavily damaged RC members can be a cost-effective solution, particularly when the repair cost remains below 40% to 50% of replacement cost [15].

In addition to economic considerations, adopting sustainable repair strategies aligns with circular economy principles. Strengthening and repairing existing RC columns reduce material waste, minimize demolition-related environmental impacts, and conserve resources. By extending the service life of structures through innovative rehabilitation techniques, the carbon footprint associated with reconstruction can be significantly lowered. The potential of repair methodologies not only enhance structural resilience but also contribute to a more sustainable built environment, as indicated in Eq. (1).

$$\frac{\mathrm{GWP}}{\mathrm{year}} = \frac{\mathrm{MQ} \times \mathrm{FR}}{\mathrm{T}} \tag{1}$$

where *GWP* (e.g., global warming potential) indicates the total climate change impact of the construction over a set period, often relative to CO_2 emissions. *MQ* is mass quantity, used in a production or system. *FR* represents the fraction released, which is a factor related to release rate (e.g., emission potential or frequency of emissions). *T* refers to the lifespan or duration over which the material's impact is being measured or calculated.

Eq. (1) estimates the annual-construction-specific *GWP* by considering the amount of the used material, the fraction of emission potential of the used material, and the time over which the *GWP* is measured. Repairing existing structures offers a significantly lower annual *GWP* compared to demolition and rebuilding. A repair-focused strategy minimizes material use (*MQ*), reduces the emission potential (*FR*) associated with new material production, and, most importantly, extends the structure's service life (*T*), thus reducing the annual GWP contribution. Prioritizing durable, targeted repairs, using low-embodied-carbon materials, and ensuring proper execution are key to maximizing the environmental benefits of repair and contributing to a more sustainable built environment. Therefore, this study presents the repair of heavilty damaged six substandard RC column specimens by CRFP. They are designed to reflect common construction deficiencies in the Mediterranean region. The full-scale tests were, first, conducted to assess the as-built behavior of the columns. Following this, the damaged specimens are repaired using carbon fiber-reinforced polymers (CFRPs) and retested under the same conditions as the as-built specimens. The results from the entire cyclic test program for both the as-built and repaired specimens are then compared to validate the repair strategy.

2 EXPERIMENTAL STUDY

The experimental setup aimed to represent real-world conditions that would induce the intended failure mechanisms in the test models. The full-scale single-curvature RC columns with a single footing were designed to reflect substandard structural building stock observed in older constructions. Key dimensional and material properties, representative of non-ductile, pre-1970s buildings with noncompliant seismic detailing, were systematically documented in Table (1).

To evaluate the influence of reinforcement details on the bond-slip response, three different lap-splice configurations were examined (Fig. 1a–c). The first configuration included columns (E1-T-H or L series, H represents a

Parameter	Mean-μ	Coeff. of Var.	Test Program	Remarks
Story height [m]	2.87*	0.10*	3.00	Single curvature test of cantilever column with a height of 1.75 m (1.50 m at loading point-story height 3.00 m)
Column width [mm]	255*	0.08*	350	Symmetrical column section is adopted
Column depth [mm]	535*	0.25*	350	
Longitudinal reinforcement steel ratio	0.96-1.14%*	0.12-0.33*	1.00%	Minimum in EN 1992-1 [16]
Reinforcing steel yield strength [MPa]	371.10[b]	0.24[b]	275	Plain round bar
Transverse reinforcement diameter [mm]	8*	0.02*	8	Plain round bar, closed hoop with 90° hook
Transverse reinforcement spacing [mm]	181.21*	0.20*	150	Selected according to construction practices
Lap splice	$50d_b$[y]	N/A	$50d_b$	From investigated blueprints
Concrete compressive strength [MPa]	16.73[b]	0.51[b]	12.29 (average of all)	Low-strength concrete with improper mix-design, poor compaction, and segregation
Axial load ratio	0.32[y]	0.53[y]	0.32 for high axial load and 0.15 for low axial load	284 observations in Istanbul, Türkiye, μ = 0.32, and μ-σ = 0.15

*Ozmen et al. [17] , [b]Bal et al. [18] , and [y]Yurdakul et al. [10]

Table 1: Target geometrical and material parameters retrieved from available literature.

high axial load ratio, while L indicates a low axial load ratio) with continuous longitudinal bars and no lap-splice length (Fig. 1a). It is important to note that the continuous reinforcement without a lap-splice (Fig. 1a) does not reflect a standard detailing practice; rather, theoretical models assume a perfect connection across the lap-splice length. The second (E1-C-H or L series) followed a conforming design, featuring a sufficient lap-splice length and hooks at the ends of the plain reinforcing steel (Fig. 1b). The third configuration (E1-NC-H or L series) was a nonconforming design, lacking hooks at the reinforcing bar ends (Fig. 1c).

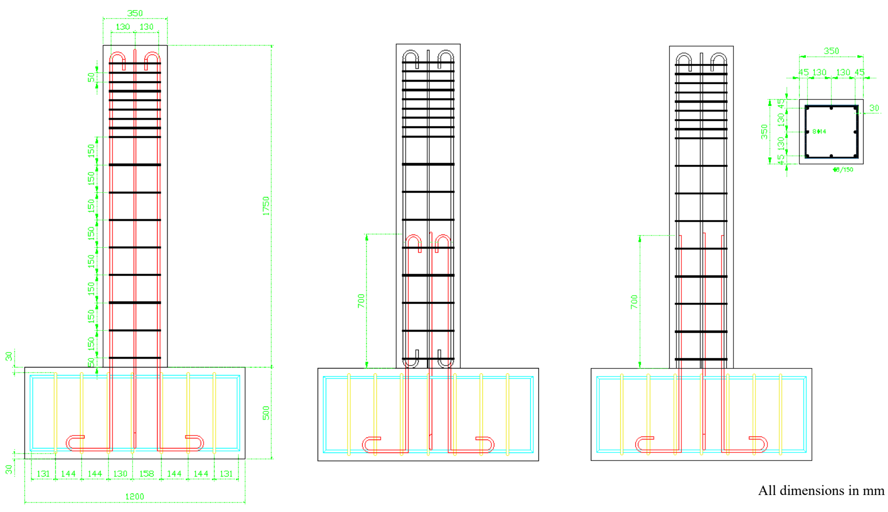

(a) (b) (c)

Figure 1: Reinforcement detail (a) continuous without lap-splice length (b) confirming configuration with hooks (c) nonconforming configuration without hooks.

During the test, the single curvature cantilever column with a clear height of 1.75 m (2.25 m including the foundation) was positioned vertically and connected to a strong floor. Two actuators, each capable of applying 630 kN while maintaining a constant axial load, were attached to the rigid beam of the loading frame. A separate actuator with a 250 kN capacity imposed lateral displacement in incremental amplitudes. To prevent out-of-plane movement, the loading beam was laterally supported (Fig. 2a and b). The cyclic tests continued until reaching a 3.85% drift ratio.

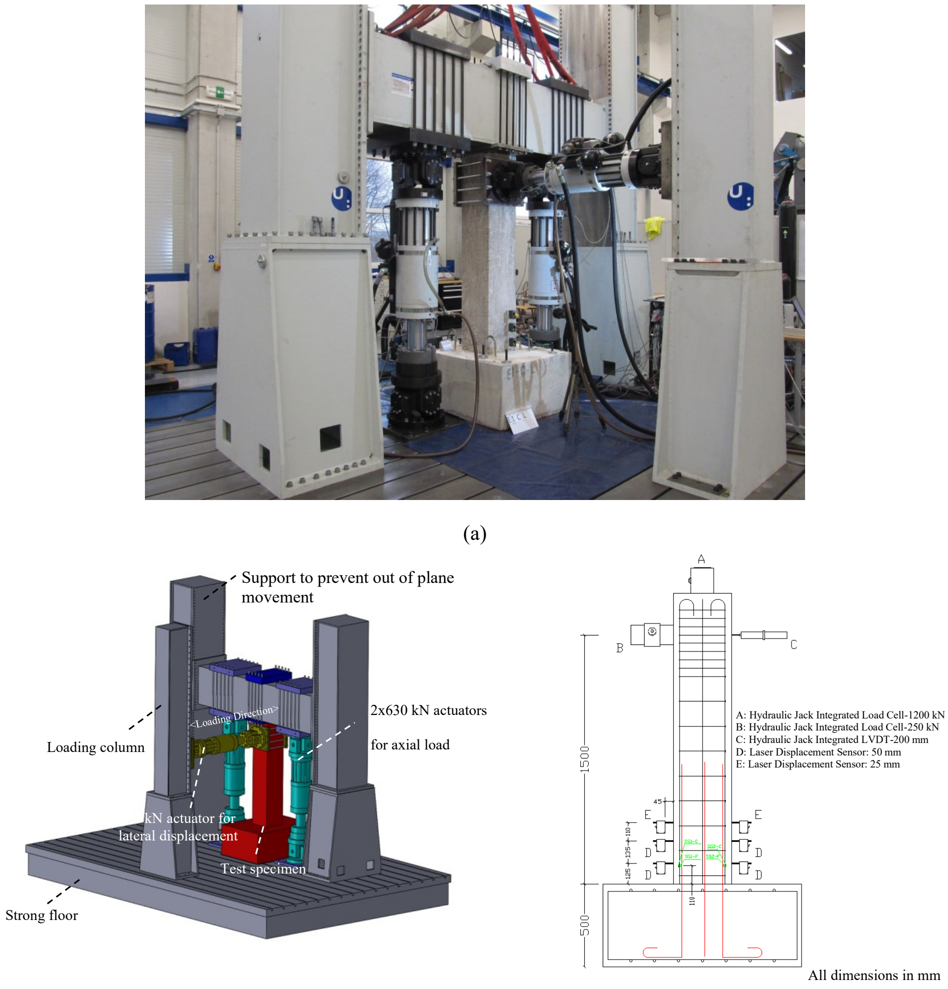

Figure 2: (a) Test stand (b) setup detail (c) instrumentations.

3 PRE-DAMAGE and REPAIR

The target ultimate inter-story drift ratio (IDR) demand imposed on the test specimens is identified as 3.85%, at which heavy structural damage is ensured by reaching a 20% strength loss. This represents the maximum level of damage achievable under the given constraints. Additionally, if visual indicators such as crack width, concrete spalling, or concrete crushing are used to assess the severity and extent of damage, it is anticipated that all specimens will develop significant cracks, with exposed or crushed reinforcing bars by the end of the tests. After testing the specimens in as-build condition, the repair process was conducted under a drift = 0 condition, with the axial load removed during the repair procedure. The flexural strength contribution of CFRP was assessed in accordance with ACI 440.2R-17 [19]. Similarly, in the shear design, the contributions of the existing shear reinforcement and concrete were disregarded. The additional shear strength required was assumed to be equivalent to the experimentally measured column shear force, and the CFRP was designed accordingly following ACI 440.2R-17 [19]. The design anchor length of CFRP spikes, used to secure the extended CFRP to the foundation, was calculated based on the methods proposed by Bournas et al. [20] and del Rey Castillo [21]. Ultimately, two layers of 300 g/m² CFRP (measuring 350 × 1625 × 0.164 mm) were applied in the longitudinal direction, while one layer of 300 g/m²

CFRP (measuring 100 × 1575 × 0.164 mm) was installed in the transverse direction at 100 mm intervals.

4 TEST RESULTS and DISCUSSIONS

The overall response of the as-built specimens was primarily governed by flexural behavior with significant reinforcement slip and axial damage. Specimens with a high axial load ratio (i.e., E1-T-H, E1-C-H, E1-NC-H) exhibited a less ductile response, with strength deterioration beginning after reaching the ultimate column shear and declining rapidly beyond the peak response (Fig. 3a–c). Initial visible flexural cracks appeared at drift levels corresponding to the ultimate column shear, followed by severe cracking, concrete crushing, and buckling of the column reinforcement (Fig. 4a–c). In contrast, specimens with a low axial load (i.e., E1-T-L, E1-C-L, E1-NC-L) displayed narrower hysteresis loops (Fig. 3d–f), indicating that bond-slip behavior was more pronounced in these cases. Additionally, lap-splice and hook details influenced the formation of flexural cracks within the expected plastic hinge region. However, rather than being evenly distributed, only a few large cracks formed within the plastic hinge length (Fig. 4d–f).

Following the repair process, the load-bearing capacity of the specimens was restored. In many cases, the recorded column shear in the repaired specimens was higher than as-build state. For repaired specimens with a low axial load, the drop in strength was less significant compared to the as-built specimens, and they maintained their ultimate lateral load capacity even in succeeding cycles. Conversely, in repaired specimens subjected to a high axial load, early cycles triggered FRP debonding. Nevertheless, the repaired specimens exhibited a progressive decline in load capacity, with a stepwise failure mechanism that increased displacement ductility demand up to a certain extent. The overall behaviour of specimens are presented in Table (2).

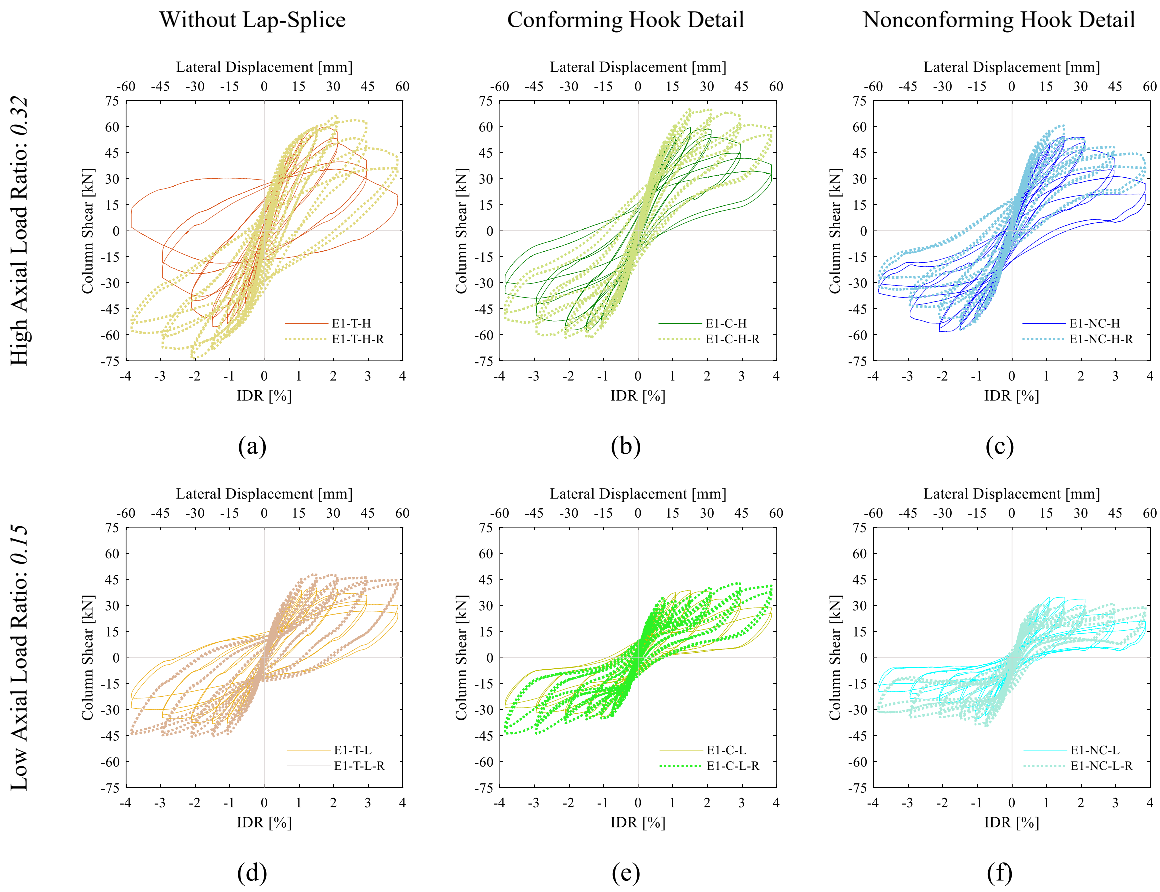

Figure 3: Cyclic response: (a) E1-T-H(R) (b) E1-C-H(R) (c) E1-NC-H(R) (d) E1-T-L(R) (e) E1-C-L(R) (f) E1-NC-L(R).

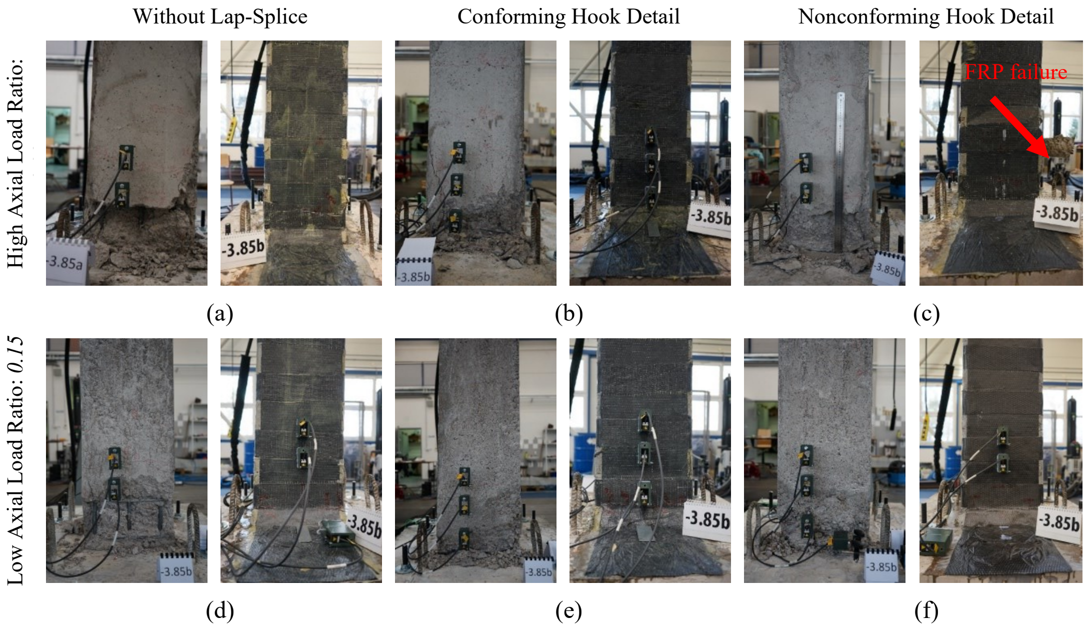

Figure 4: Damage pattern at the end of the test: (a) E1-T-H(R) (b) E1-C-H(R) (c) E1-NC-H(R) (d) E1-T-L(R) (e) E1-C-L(R) (f) E1-NC-L(R).

Remarks	E1-T-H(R)	E1-C-H(R)	E1-NC-H(R)	El-T-L(R)	E1-C-L(R)	E1-NC-L(R)
Interface Crack	0.55a%	0.39a%	0.39a%	0.28a%	0.28b%	0.28a%
Flexural Crack	1.08b% (0.35 mm at about 180 mm and 340 mm from column base)	1.51a% (0.35 mm at about 350 mm, 0.15 mm at about 480 mm)	1.51a% (0.15 mm at about 350 mm, 0.10 mm at about 240 mm)	0.77a% (0.20 mm at about 120 mm and 260 mm)	0.77a% (0.20 mm at about 110 mm and 255 mm)	0.77a% (0.20 mm at about 125 mm and 260 mm)
Concrete Spalling	2.11a%	1.08a	2.11a%	2.95b%	2.95b%	2.95a%
Reinforcement Yielding	1.08a%	1.51a%	1.51a%	1.08a%	1.08a%	1.08a%
Reinforcement Buckling	3.85a%	3.85a%	3.85a%	3.85a%	- -	- -
State at the end of the test	Concrete crushing with reinforcement buckling, heavy damage up to 240 mm from the column base	Concrete crushing with slight reinforcement buckling and interface opening about 8 mm	Concrete crushing with slight reinforcement buckling and interface opening about 12 mm	Concrete crushing with reinforcement buckling and heavy damage up to 240 mm from the column base	Local concrete crushing near the interface and interface opening about 15 mm	Local concrete crushing near the interface and interface opening about 18 mm
Repaired performance	Recovered strength and enhanced ductility	Recovered strength and enhanced ductility	Recovered strength and enhanced ductility	Recovered strength	Recovered strength	Recovered strength
State of the repaired specimen	Partial FRP fracture in longitudinal direction	Partial FRP fracture in longitudinal direction	FRP fracture in transverse direction	Partial FRP fracture in longitudinal direction	Partial FRP fracture in longitudinal direction	Partial FRP fracture in longitudinal direction

Table 2: Summary of test results.

5 CONCLUSIONS

This study emphasizes the importance of sustainable repair techniques in supporting the circular economy, particularly for substandard RC structures. By focusing on the repair of heavily damaged substandard RC columns using CFRPs, this study investigates innovative repair methods that recover the former capacity and extend the service life of RC columns. These approaches help conserve resources, reduce the carbon footprint of reconstruction, and contribute to a more sustainable built environment. The study begins with full-scale testing to assess the behavior of six substandard RC columns in their original condition. Following this, the damaged columns are repaired using CFRPs and retested under the same conditions as the initial tests. By comparing the results from the cyclic testing of both the as-built and repaired specimens, the study validates the effectiveness of the CFRP-based repair strategy. Ultimately, this research highlights the dual benefits of such repair methods—not only improving structural resilience but also advancing sustainability in construction practices.

Based on the results of the conducted study, the following conclusions were drawn:

- The as-built specimens, which are substandard RC columns according to current design codes and standards, demonstrated poor performance. Constructed with low-strength concrete and lacking proper reinforcement details, the specimens suffered severe damage. The failure mode observed was primarily flexural, accompanied by considerable reinforcement slip and axial damage (concrete crushing and rebar buckling) in all of the specimens.
- Compared to the specimens with a low axial load ratio (i.e., 0.15), the ones with a high axial load ratio (i.e., 0.32) experienced significant axial damage, with concrete crushing and reinforcement buckling being the ultimate stages of damage.
- Following successful repair using the proposed method, the heavily damaged specimens regained their original capacities. The crack patterns and damage progression in the repaired specimens was limited compared to as-built configuration.
- The authors acknowledge that high residual deformations, which could negatively impact the overall functionality of the building, are critical factors to consider when making the repair decisions. When a building undergoes significant permanent drifts at a global scale, repair decisions for RC columns should be made carefully. Emphasizing the need to account for the limited deformation capacity of structural components in deficient RC buildings is essential when developing a practical local retrofit strategy.

6 ACKNOWLEDGMENT

This study has been accomplished with the support of the University of Pardubice under project no: Excellent Team-51030/25/DO252022.

We would also like to express our gratitude to Mr. Martin Rehak for his valuable support and contributions during test preperation.

REFERENCES

[1] Ö. Yurdakul, C. Del Vecchio, M. Di Ludovico, Ö. Avşar, Numerical simulation of substandard beam-column joints with different failure mechanisms, *Structural Concrete*, **2020**, 1–18, https://doi.org/10.1002/suco.201900003.

[2] Ö. Yurdakul, C. Del Vecchio, M. Di Ludovico, Ö. Avşar, A. Prota, Fragility functions for fiber-reinforced polymers strengthened reinforced concrete beam-column joints, *Engineering Structures*, **279**, 115570, 2023, https://doi.org/10.1016/j.engstruct.2022.115570.

[3] Ö. Yurdakul, C. Del Vecchio, M. Di Ludovico, L. Routil, Ö. Avşar, Crack width-based fragility curves for repairability of substandard beam-column joints, *Bulletin of Earthquake Engineering*, **19**, 6081–6111, 2021, https://doi.org/10.1007/s10518-021-01218-6.

[4] S. Angster, E.J. Fielding, S. Wesnousky, I. Pierce, D. Chamlagain, D. Gautam, et al., Field reconnaissance after the 25 April 2015 M 7.8 Gorkha Earthquake, *Seismological Research Letters*, **86**, 1506–1513, 2015, https://doi.org/10.1785/0220150135.

[5] A. Kc, K. Sharma, B. Pokharel, Performance of heritage structures during the Nepal Earthquake of April 25, 2015, *Journal of Earthquake Engineering*, **23**, 1346–1384, 2019, https://doi.org/10.1080/13632469.2017.1360225.

[6] Ö. Yurdakul, B. Duran, O. Tunaboyu, Ö. Avşar, Field reconnaissance on seismic performance of RC buildings after the January 24, 2020 Elazığ-Sivrice earthquake, *Natural Hazards*, **105**, 859–887, 2021, https://doi.org/10.1007/s11069-020-04340-x.

[7] D. Biskinis, M.N. Fardis, Effect of lap splices on flexural resistance and cyclic deformation capacity of RC members, *BUST*, **102**, 51–59, 2007, https://doi.org/10.1002/best.200710105.

[8] G.M. Verderame, G. Fabbrocino, G. Manfredi, Seismic response of r.c. columns with smooth reinforcement. Part II: Cyclic tests, *Engineering Structures*, **30**, 2289–2300, 2008, https://doi.org/10.1016/j.engstruct.2008.01.024.

[9] H. Rodrigues, H. Varum, A. Arêde, A.G. Costa, Behaviour of reinforced concrete column under biaxial cyclic loading—state of the art, *International Journal of Advanced Structural Engineering*, **5**, 4, 2013, https://doi.org/10.1186/2008-6695-5-4.

[10] Ö. Yurdakul, P. Vnenk, L. Routil, B. Culek, Ö. Avşar, Post-damage recovery of substandard RC columns by CFRPs, *Engineering Structures*, **306**, 117806, 2024, https://doi.org/10.1016/j.engstruct.2024.117806.

[11] M. Parker, D. Steenkamp, The economic impact of the Canterbury earthquakes, *Reserve Bank of New Zealand: Bulletin*, **75**, 2012.

[12] G. Di Pietro, T. Mora, The effect of the L'Aquila earthquake on labour market outcomes, *Environment and Planning C: Government and Policy*, **33**, 239–255, 2015, https://doi.org/10.1068/c12121r.

[13] AFAD, Afet Raporu-Van Depremi, Disaster and Emergency Management Presidency, Ministry of Interior, Türkiye, 2012, Retrieved from: https://www.afad.gov.tr/odenekler-harcamalar-kampanyalar.

[14] SBB, 2023 Kahramanmaraş and Hatay earthquakes report, Presidency of Strategy and Budget, Türkiye, 2023, Available at: https://www.sbb.gov.tr/wp-content/uploads/2023/03/2023-Kahramanmaras-and-Hatay-Earthquakes-Report.pdf.

[15] H.H. Aydoğdu, *Strategies for Seismic Risk Mitigation by Considering Economic Criteria on a Regional Basis*, Ph.D. Thesis, Department of Earthquake Engineering, Istanbul Technical University, Türkiye.

[16] CEN, Eurocode 2: Design of concrete structures - Part 1-1: General rules and rules for buildings, *EN 1992-1-1*, Comité Européen de Normalisation (CEN), Brussels, Belgium, 2004.

[17] H.B. Ozmen, M. Inel, S.M. Senel, A.H. Kayhan, Load carrying system characteristics of existing Turkish RC building stock, *International Journal of Civil Engineering*, **13**, 16, 2015.

[18] İ.E. Bal, H. Crowley, R. Pinho, F.G. Gülay, Detailed assessment of structural characteristics of Turkish RC building stock for loss assessment models, *Soil Dynamics and Earthquake Engineering*, **28**, 914–932, 2008, https://doi.org/10.1016/j.soildyn.2007.10.005.

[19] ACI 440.2R-17, Guide for the design and construction of externally bonded FRP systems for strengthening concrete structures, *ACI 440.2R-17*, American Concrete Institute, USA, 2017.

[20] D.A. Bournas, A. Pavese, W. Tizani, Tensile capacity of FRP anchors in connecting FRP and TRM sheets to concrete, *Engineering Structures*, **82**, 72–81, 2015, https://doi.org/10.1016/j.engstruct.2014.10.031.

[21] E. del Rey Castillo, R. Kanitkar, S.T. Smith, M.C. Griffith, J.M. Ingham, Design approach for FRP spike anchors in FRP-strengthened RC structures, *Composite Structures*, **214**, 23–33, 2019, https://doi.org/10.1016/j.compstruct.2019.01.100.